Journal of Statistical Physics, Vol. 43, Nos. 5/6, 1986

Monte Carlo Studies of Nuclear Many-Particle Systems

J. W. Negele[1]

Stochastic evaluation of path integrals provides a useful tool for the study of a variety of nuclear systems which are otherwise not amenable to definitive analysis through perturbative, variational, or stationary-phase approximations. Ground state properties of potential models, such as quantum fluctuations in the density, are examined. Tunneling problems in quantum many-particle systems, such as spontaneous fission and the ground state structure of systems with degenerate vacuua are treated by incorporating one's physical understanding of the essential collective degrees of freedom in the stochastic algorithm. The role of subnuclear degrees of freedom is studied by comparing the exact solution of a simple confining quark model with the solution to a phase-shift equivalent hadronic potential model.

KEY WORDS: Path-integral Monte Carlo; tunneling in many degrees of freedom: fission; solution of confining quark model.

1. INTRODUCTION

Path integrals provide a useful physical perspective from which to approach Monte Carlo studies of quantum systems with many degrees of freedom. This approach retains the physical insight provided by summing over time histories, and the Monte Carlo method may be viewed simply as an alternative to the stationary-phase approximation for summing all the fluctuations around the stationary paths. It has the advantage that one may directly exploit the usual freedom in formulating path integrals for

This work is supported in part through funds provided by the U.S. Department of Energy (D.O.E.) under contract number DE-AC02-76ERO3069.

[1] Center for Theoretical Physics, Laboratory for Nuclear Science and Department of Physics, Massachusetts Institute of Technology, Cambridge, Massachusetts 02139 U.S.A.

0022-4715/86/0600-0991$05.00/0

quantal systems and utilize one's physical understanding of stationary solutions such as instantons. It therefore provides a natural perspective from which to develop stochastic methods which incorporate as much physics as possible. Relative to the Green's function Monte Carlo method described by Kalos and Ceperley (see Ref. 1 and in contributions to this conference) the path-integral Monte Carlo method has the apparent disadvantage of requiring an extrapolation in the time step size $\Delta\tau \to 0$, and the compensating advantage that for any fixed $\Delta\tau$ evolution is simpler and more efficient. In practical calculations, the two methods are roughly comparable.

To distinguish the nuclear physics problems discussed in this work from applications in other fields, it is useful to summarize the salient features of the nuclear many-body problem.

One crucial feature is the presence of diverse physical scales. The nucleon–nucleon interaction is strongly repulsive at separations less than 0.5 fm and strongly attractive in the region of 1 fm so that the range of rapid variation of the potential is characterized by $\Delta x \sim 0.2$ fm. Since a heavy nucleus has a radius of the order of 7 fm and a diffuse surface, it must be calculated in a box of linear dimension at least $L \sim 20$ fm on a side. These values of Δx and L imply that if the nuclear many-body problems were to be formulated on a lattice, for example using a functional integral over an auxiliary field, the lattice must have $(10)^3$ spatial points.

A conservative estimate of the time mesh size required to approach the continuum limit is obtained by requiring that the distance a particle evolves under the kinetic energy operator in time $\Delta\tau$ be small compared with the characteristic scale of variation of the potential Δx so that

$$\Delta\tau < \frac{m(\Delta x)^2}{2} \sim 5 \times 10^{-4}\ \mathrm{MeV}^{-1}$$

To evaluate ground state properties, we need $\beta\Delta E \gg 1$, where ΔE is the excitation energy of the first excited state. Even for nuclei with no low energy collective excitations $\beta < (1/2\ \mathrm{MeV})$ requiring 1000 time steps, and for a rotational band in which the first excited state is ~ 200 keV, an additional order of magnitude is required. Thus, description of a heavy nucleus on a space-time lattice would require $(100)^3 \times 1000$ sites, which is four to five orders of magnitude more than any lattice gauge calculation and totally prohibitive on any foreseable computer. This diversity of physical scales may be stated equivalently in terms of energies. One seeks a Monte Carlo method which simultaneously treats the dynamics of short range correlations with energies of the order of hundreds of MeV, single particle excitations of order 10 MeV, and collective effects as low as a fraction of an MeV.

In addition to diverse energy scales, we must also address the physics of substructure. Whereas some aspects of subnuclear structure may be described by meson degrees of freedom, we must ultimately understand the role of quark and gluon degrees of freedom in nuclear structure. On the one hand, we need to understand how a low-energy effective Hamiltonian in hadron degrees of freedom arises from the underlying theory and why potential theories yield such a quantitatively accurate description of energies, densities, structure, and reactions. On the other hand, we wish to understand signatures of substructure, such as the EMC effect, which tells us how the distribution of quarks in a nucleon within a nucleus differs from that in an isolated nucleon. Clearly, when the lattices used for Monte Carlo studies QCD can barely contain a proton and only qualitatively reproduce the observed hadron spectrum, we are far from bringing the tools of quantum Monte Carlo to bear directly on realistic calculations of nuclear substructure.

This hard assessment of the scope of the problems posed by diverse physical scales and by quark–gluon substructure clearly indicates that for the present, Monte Carlo studies in nuclear physics must concentrate on pedagogical models rather than definitive realistic calculations. In the remainder of this paper, I explain how our understanding of some of the underlying physics is incorporated in stochastic calculations and discuss what is being learned from studies of models.

2. FREEDOM IN FORMULATING STOCHASTIC METHODS

As is evident from the great diversity of approaches discussed at this conference, there is a tremendous amount of freedom in formulating Monte Carlo methods to study many-body problems. The principal intellectual challenge, therefore, is to exploit this freedom and to utilize one's physical insight to incorporate as much of the essential physics of the problem as possible into the stochastic algorithm.

There are three primary categories of choices which will be discussed here: the physical quantity to calculate, the functional integral representation used to formulate the path integral, and the choice between sampling the global action or solving an initial-value diffusion problem.

The first question is what physical quantity to evaluate. One option is the trace of the evolution operator $\sum_n \langle n | e^{-\beta H} | n \rangle$, which provides all thermodynamic information at inverse temperature β. Whereas this is obviously useful for a system that is in thermodynamic equilibrium, it precludes incorporating knowledge of the structure of a specific state. A second option treated in detail below is to choose a specific matrix element

of $e^{-\beta H}$ which is optimal for calculation of a particular observable.[2,3] For example, in the limit of large β, the ground state energy may be written

$$E = \frac{\langle \phi | He^{-\beta H} | \phi \rangle}{\langle \phi | e^{-\beta H} | \phi \rangle} \tag{2.1}$$

where $|\phi\rangle$ is an approximate wave function. The expectation value of an operator $\mathcal{O}$ may be written exactly as

$$\begin{aligned} \langle \mathcal{O} \rangle &= \frac{\langle \phi | e^{-\beta H} \mathcal{O} e^{-\beta H} | \phi \rangle}{\langle \phi | e^{-2\beta H} | \phi \rangle} \\ &\approx 2 \frac{\langle \phi | \mathcal{O} e^{-\beta H} | \phi \rangle}{\langle | e^{-\beta h} | \phi \rangle} - \frac{\langle \phi | \mathcal{O} | \phi \rangle}{\langle \phi | \phi \rangle} \end{aligned} \tag{2.2}$$

The phase shift for the scattering of two composite particles at energies below the excitation threshold for the first excited state is obtained by imposing the boundary condition that the wave functions vanish at a specified fragment separation distance and evaluating the energy E of the total system as a function of this distance.[4] The fission lifetime may be calculated, exactly, below the threshold for fragment excitation by calculating the scattering phase shift it may be calculated, approximately, for any high barrier by calculating the overlap matrix element V between interior and exterior states[5]

$$\frac{\langle \phi_{\text{int}} | e^{\beta H} | \phi_{\text{ext}} \rangle}{[\langle \phi_{\text{int}} | e^{-\beta H} | \phi_{\text{int}} \rangle \langle \phi_{\text{ext}} | e^{-\beta H} | \phi_{\text{ext}} \rangle]^{1/2}} = \tan \text{h}(V\beta) \tag{2.3}$$

A second choice is the functional integral representation.[6] Different. yet exact, functional integrals may be obtained by inserting alternative resolutions of unity at each time step: integrals over coordinate states, alternate integrate over coordinate and momentum states, boson coherent states, overcomplete sets of Slater determinants, and Grassman coherent states, to name a few. Alternatively, by applying the Hubbard–Stratonovich transformation, the many-body evolution operator may be expressed as an integral over an auxiliary field of a one-body evolution operator. Whereas each form has its distinct advantages and limitations, in view of the exceedingly large mesh size necessitated by the behavior of the nuclear force for any functional integral over fields, the Feynman path integral in coordinate representation is most suitable for our present purposes.

Finally, the last question is whether to repeatedly sample the action for the system, thereby generating a sequence of complete time histories, or to formulate an initial value problem in which an initial ensemble of

points is evolved in time to generate an ensemble of time histories. It is particularly appropriate to discuss sampling the action at this meeting honoring Nic Metropolis on the occasion of his seventieth birthday, since application of the celebrated method of Metropolis et al.[7] provides an extremely satisfying physical treatment of tunneling problems described in the next section.

The initial value formulation offers the opportunity to incorporate any understanding one has of the behavior of the wave function directly in the random walk. The basic idea of this initial value random walk is simple. Let us decompose the infinitesimal evolution operator into the product of a Gaussian probability and a residual weight as follows

$$\begin{aligned} \langle x_n | \, e^{-\varepsilon(\hat{H}-E)} \, | x_{n-1} \rangle &\approx \sqrt{\frac{m}{2\pi\varepsilon}} \, e^{-(m/2\varepsilon)(x_n - x_{n-1})^2} \, e^{-\varepsilon[V(x_{n-1})-E]} \\ &\equiv P(x_n, x_{n-1}) \, W(x_{n-1}) \end{aligned} \tag{2.4}$$

so that

$$\begin{aligned} &\langle \phi_a | \, e^{-\beta(H-E)} \, | \phi_b \rangle \\ &\quad = \int dx_1, \ldots, dx_1 \, \phi_a(x_n) \, P(x_n, x_{n-1}) \\ &\qquad \times W(x_{n-1}), \ldots, P(x_3, x_2) \, W(x_2) \, P(x_2, x_1) \, W(x_1) \, \phi_b(x_1) \end{aligned} \tag{2.5}$$

This product of probabilities and weights is evaluated as follows. First, x_1 is randomly selected according to the distribution function $\phi_b(x_1)$, which may be chosen to be positive, and the temporary value of the score is defined to be $W(x_1)$. Given x_1, x_2 is chosen to be Gaussian-distributed about x_1 according to the probability $P(x_2, x_1)$, and the score is multiplied by $W(x_2)$. This procedure is repeated for all n; finally x_n is chosen to be Gaussian-distributed about $x_n - 1$ and the score is multiplied by $\phi_a(x_n)$. For an ensemble of such calculations, each score $\phi_a(x_n) \prod_{i=1}^{n-1} W(x_i)$ is obtained with probability $\prod_{i=1}^{n-1} P(x_{i+1}, x_i) \, \phi_b(x_1)$ so that the average value of the score for a large ensemble of random samples approaches $\langle \phi_a | \, e^{-\beta(H-E)} \, | \phi_b \rangle$.

The statistical accuracy of this basic method may be improved greatly by replicating points at each step with probability proportional to $W(x_n)$ instead of accumulating the weight $W(x_n)$ in the score. The calculation may then be viewed as a diffusion process with a source-sink term $W(x)$ and diffusion term $P(x_m, x_{m-1})$. An initial ensemble of points $\{x^i\}$ distributed according to $\phi_b(x)$ is first diffused by the Gaussian $P(x_2, x_1)$. In regions where $V(x) > E$, $W(x^i) < 1$ and the point x^i is deleted from the ensemble with probability $1 - W(x^i)$. When $W(x^i) > 1$, the point x^i is always

replicated $[W(x^i)]$ times (where $[W]$ denotes the greatest integer in W) and with probability $W(x^i) - [W(x^i)]$ it is replicated one additional time. In each successive step, points diffuse according to $P(x^i_m, x^i_{m-1})$ and are replicated according to $W(x^i_m)$. Thus, elements of the ensemble are created in regions of attractive $V-E$ and deleted in regions of repulsive $V-E$ such that the final ensemble of points $\{x_n\}$ is distributed according to $\prod_{m-1}^{n-1} P(x_{m+1}, x_m)\, W(x_i)\, \phi(x_i)$ and $\langle \phi_a | e^{-\beta(H-E)} | \phi_a \rangle$ is given by the average value of $\phi_a(x)$ evaluated with the ensemble $\{x_n\}$. Whereas the first method retains ensembles having products of weights $\prod_{i=1}^{n} W(x_i)$ which may vary over many order of magnitude with corresponding loss of statistical accuracy, in the replication method each member of the final ensemble $\{x_n\}$ contributes with the same weight. In practice, the value of E is selected to maintain a constant average ensemble size and yields an independent evaluation of the ground state energy.

A major improvement in the initial value problem is to guide the random walk using an approximate trial wave function $\phi(x)$ which contains as much of the essential physics as may be understood at the outset. The infinitesimal evolution operator for the product $\phi(x)\,\psi(x)$ is $\phi(\hat{x})\, e^{-\varepsilon H(\hat{x})}[1/\phi(\hat{x})]$, which to leading order in ε has the matrix element

$$\langle x_n | \phi(\hat{x})\, e^{-\varepsilon(\hat{H}-E)} \frac{1}{\phi(\hat{x})} | x_{n-1} \rangle$$

$$= \sqrt{\frac{m}{2\phi\hat{\varepsilon}(x_{n-1})}}\, e^{[m/2\hat{\varepsilon}(x_{n-1})](x_n - x_{n-1} - (\varepsilon/m)[\phi'(x_{n-1})/\phi(x_{n-1})])^2}$$

$$\times e^{-\varepsilon[[-(1/2m)\phi''(x_{n-1}) + V(x_{n-1})\phi(x_{n-1})]/\phi(x_{n-1})]} \tag{2.6}$$

This evolution operator differs from (2.4) in three respects. The Gaussian diffusion term is shifted by a drift term proportional to ϕ'/ϕ, which guides members of the ensemble away from regions where the wave function is small so that the points sample most densely the region in which the contribution in the largest. The source-sink term is now $(H-E)\,\phi/\phi$ instead of $V-E$. In the limit in which ϕ is exact, this term is just a constant, there are no fluctuations in the population, all the physics is contained in the drift term, and the statistical variance is a minimum. To the extent to which ϕ incorporates much of the essential physics, the evolution is guided by that portion of the physics through the drift term, and the stochastic treatment of the source term is only required to treat the remnant of the physics which is left out of the trial function. Finally, in principle, the size of the Gaussian step $\hat{\varepsilon}(x_{n-1})$ depends upon x_{n-1},

$$\hat{\varepsilon}(x) = \varepsilon \left[1 - \frac{\varepsilon}{m} \frac{d^2}{dx^2} \ln \phi(x) \right]^{-1}$$

although in the special case of an oscillator, this yields an irrelevant scale factor and in most practical applications the effect is negligible.[8] Trial functions have been utilized extensively in the closely related Greens function Monte Carlo method, and in a variety of physical applications are absolutely necessary to render a calculation practical.[1] More generally,[9] a time-dependent trial function $\phi(x, t)$ may be used to guide the random walk in evaluating the matrix element $\langle \phi_b | e^{-\beta H} | \phi_a \rangle$. In this case the source-sink term is $[(\partial/\partial r + H)/\phi]\,\phi$ so that the optimal choice is the time reverse of the solution to the imaginary time Schrödinger equation with the initial condition $\phi = \phi_b$.

The many-fermion problem may be treated formally in the same way as the one-body problem. The matrix element of the infinitesimal evolution operator between antisymmetrized states is

$$\langle x_1^n \cdots x_A^n | \, \phi e^{-\varepsilon(\hat{H}-E)} \frac{1}{\phi} | x_1^{n-1}, \ldots, x_A^{n-1} \rangle$$

$$= \sum_P (-1)^P \left[\frac{m}{2\pi\hat{\varepsilon}}\right]^{A/2} e^{-(m/2\hat{\varepsilon})(x_{Pi}^n - x_i^{n-1} - D_i(x^{n-1}))^2 - \varepsilon S(x^{n-1})} \tag{2.7}$$

where the drift term is

$$D_i(x^{n-1}) = \frac{\varepsilon}{m} \frac{d}{dx_i^{n-1}} \ln \phi(x_1^{n-1}, \ldots, x_A^{n-1})$$

and the source term is

$$S(x^{n-1}) = \frac{(\hat{H} - E)\,\phi(x^{n-1})}{\phi(x^{n-1})}$$

In more than one spatial dimension, interference between positive and negative contributions to the functional integral degrades the statistical accuracy such that very good trial functions and exceedingly large ensembles are required to obtain useful results.[10] In one dimension, however, antisymmetry completely specifies the nodal points and a positive definite result may be obtained by simply evolving the wavefunction in the subspace $x_1 < x_2 < x_3, \ldots, x_A$. As described in Ref. 3, it is useful to approximate the determinant by

$$\sum_P (-1)\, P e^{-(m/2\varepsilon)(x_{Pi}^n - x_i^{n-1} - D_i)^2}$$

$$= e^{-(m/2\varepsilon)\sum_i (x_i^n - x_i^{n-1} - D_i)^2} \det \left| e^{-(m/2\varepsilon)[(x_i^n - x_j^{n-1} - D_j)^2 - (x_i^n - x_i^{n-1} - D_i)^2]} \right|$$

$$\approx e^{-(m/2\varepsilon)\sum_i (x_i^n - x_i^{n-1} - D_i)^2} \prod_{i=2}^{A} (1 - e^{-(m/\varepsilon)(x_i^n - x_{i-1}^n)(x_i^{n-1} - D_i - x_{i-1}^{n-1} + D_{i-1})}) \tag{2.8}$$

which includes the effect of the first images surrounding each node.

3. TUNNELING

Tunneling in systems with many degrees of freedom arises in many areas of physics. Although this work was motivated by problems such as spontaneous and induced fission and subbarrier fusion in nuclear physics, similar problems abound in many disciplines: tunneling in solid state devices, the contribution of cyclic permutations to the ground state energy of solid[3] HE systems with multiply degenerate vacuua in field theory, and a rich variety of molecular and biological systems.

The usual approximation for these tunneling problems is reduction to a one-body problem with an effective mass and effective potential. Such a reduction necessarily involves the imposition or derivation of a collective variable. Although the theory includes the average effects of other degrees of freedom, it cannot include direct coupling to them.

Path integrals provide a natural and convenient framework for addressing tunneling in systems with many degrees of freedom. A great deal of physical insight into this tunneling has been obtained by application of the stationary phase approximation to an appropriately formulated path integral. The basic idea developed by Langer,[11] Polyakov,[12] and Coleman[13] is to find the appropriate stationary path, referred to as a "bubble," "instanton," or "bounce," which connects the two relevant classically allowed regimes. In this section, I will sketch the basic ideas, described in detail elsewhere,[14,5] of how this qualitative physics is incorporated in a Monte Carlo calculation.

Tunneling Observables with Euclidean Data Integrals

In real time, the evolution of probability out of the region of a metastable state directly specifies the lifetime of a metastable state. After Wick rotation to imaginary time, which is necessary in order to obtain a real path integral amenable to Monte Carlo evaluation, evolution of the wave function through the barrier is no longer directly related to the lifetime, so we formulate an appropriate imaginary time observable from which the lifetime may be extracted.

The first question is thus how to calculate the lifetime of a metastable state in terms of a Euclidean path integral. The basic idea that we use is sketched for a one-dimensional barrier in Fig. 1. The lowest eigenstate in the potential $V(x)$ with an infinite wall at a corresponds to a scattering wave function in the full domain with the same energy having a node at a. Since E specifies the momentum k and a specifies the phase shift δ,

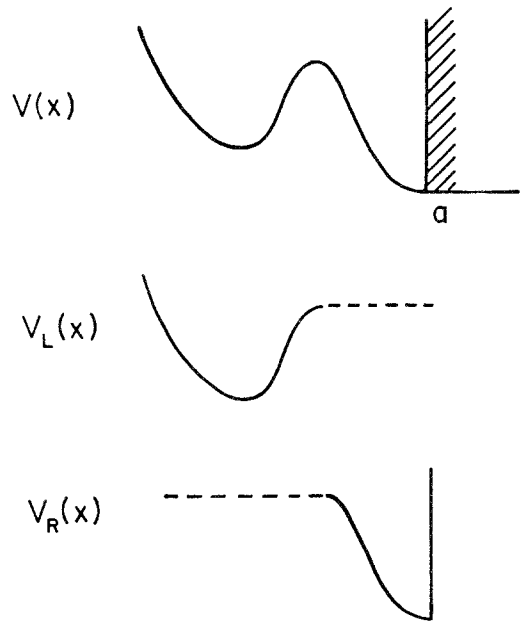

Fig. 1. Potential for a metastable state in one dimension.

calculating the energy $E^{(1)}(a)$ of the lowest eigenfunction as a function of the wall position a, in principle, specifies $\delta(k)$ and thus the lifetime

$$\delta(k) = \delta_0 + bk + \tan^{-1}(\gamma/k_0 - k) \tag{3.1}$$

where $\gamma = (m/2k_0)\,\Gamma$.

For the high barriers and long lifetimes of interest in this work, it is impractical to calculate $\delta(k)$ to sufficient precision to evaluate γ, so it is perferable to relate γ to the splitting of two degenerate ground states. Thus, let us decompose $V(r)$ into the left and right wells sketched in Fig. 1 and adjust a such that $E_L = E_R$. Then, one mayshow, either by using the bound state condition $\delta(k) = n\pi - ka$ or the Kohn variational principle, that

$$\gamma = -\frac{m}{4(dE/da)}(\Delta E)^2 \,|_{E_L = E_R}\left(1 + \mathcal{O}\frac{\gamma}{k_0}\right) \tag{3.2}$$

where ΔE is the energy splitting between the two lowest states in the degenerate double well. Note that this result has the form expected from the Fermi Golden Rule of a transition matrix element squared (since $\Delta E \sim \langle \phi_L |\, \Delta v \,| \phi_R \rangle$) times a density of states [related to $(dE/da)^{-1}$].

The next question is how to evaluate ΔE. It is prefereable to use a

quantity which is dominated by paths connecting the left and right wells, and the most satisfactory quantity we have found is the ratio

$$R = \frac{\langle \phi_L | \, e^{\beta H} \, | \phi_R \rangle}{[\langle \phi_L | \, e^{-\beta H} \, | \phi_L \rangle \langle \phi_R | \, e^{-\beta H} \, | \phi_R \rangle]^{1/2}} \tag{3.3}$$

where ϕ_L and ϕ_R are trial wave functions localized in the left and right wells, respectively. For the special case of a symmetrical well with the definition $\alpha \equiv (\langle 1 | \phi_L \rangle / \langle 0 | \phi_L \rangle)^2$

$$R \xrightarrow[\beta(E_2 - E_0) \gg 1]{} \frac{1 - \alpha e^{-\beta \Delta E}}{1 + \alpha e^{-\beta \Delta E}} = \tan h \left(\frac{\beta \Delta E - \ln \alpha}{2} \right) \tag{3.4}$$

Hence, the constant ΔE may be obtained by calculating

$$\Delta E_{\text{eff}}(\beta) \equiv \frac{2 \tan h^{-1} R}{\beta} = \Delta E - \frac{\ln \alpha}{\beta} \tag{3.5}$$

at several values of β and separating the $1/\beta$ correction.

Stochastic Calculation of Tunneling with One Degree of Freedom

The essential difficulties encountered in tunneling problems and their solutions may be illustrated for the case of the symmetric double well

$$\left[-\frac{1}{2m} \frac{d^2}{dx^2} + (x^2 - 1)^2 \right] \psi = \varepsilon \psi \tag{3.6}$$

The spatial coordinate has been scaled such that the minima occur at $x = \pm 1$ and the energy has been scaled such that the barrier height is 1, so that the penetrability of the barrier is controlled by m. For orientation, it is useful to note the properties of the instantion solution which satisfies the classical equations of motion in the inverted well

$$x(\tau) = \tan h \gamma \tau \tag{3.7}$$

with $\gamma = \sqrt{2/m}$ leading to an approximate splitting

$$\Delta E = 2\kappa e^{-S_0} \tag{3.8}$$

where $S_0 = \frac{4}{3}\sqrt{2m}$ and $\kappa = (4\sqrt{2}/\sqrt{\pi})(8/m)^{1/4}$. In the dilute instanton gas approximation, the probability of a configuration containing n instantons is $P(n) = [(\beta\kappa)^n e^{-nS_0}]/n!$. The harmonic approximation about the minima

yields a harmonic oscillator energy $\frac{1}{2}\omega = \sqrt{2/m}$. For mass $m = 4$, $E_0 = .572$ compared with $\omega/2 = .707$, and $E_1 - E_2 = .116$ compared with $\Delta E \sim .175$ from (14) so that this mass corresponds to a low barrier. In contrast, $m = 12$ corresponds to a high barrier; $E_0 = .381$ is comparable to the harmonic result $\omega/2 = .408$, and the instanton approximation $\Delta E \sim 0.0084$ is reasonably close to the small splitting 0.0089.

The Feynman path integral

$$\langle x_n | e^{-\beta H} | x_0 \rangle = \int dx_{n-1}, \ldots, dx_1 \prod_{i=1}^{N} e^{-(m(x_i - x_{i-1})^2/2\varepsilon) - (V(x_i) + V(x_{i-1})/2)\varepsilon} \tag{3.9}$$

is evaluated by using the Metropolis[7] algorithm to sample the action.

A Markov chain of configurations $\{\vec{x}^{(1)}, \vec{x}^{(2)}, \ldots, \}$ is generated by a rule $P(\vec{x}^{(n)} \to \vec{x}^{(n+1)})$ specifying the probability of obtaining $\vec{x}^{(n+1)}$ from $\vec{x}^{(n)}$ and satisfying the microreversibility requirement $e^{-S(x)} P(\vec{x} \to \vec{y}) = e^{-S(y)} P(\vec{y} \to \vec{x})$. In the form we use here, a tentative configuration, $\vec{x}_T$, is generated according to some convenient symmetrical rule $F(\vec{x} \to \vec{x}_T) = F(\vec{x}_T \to x)$. Then, if $\Delta S \equiv S(\vec{x}_T) - S(\vec{x}) \leqslant 0$ this tentative configuration is accepted, that is, $\vec{y} \equiv \vec{x}_T$. If $\Delta S > 0$, the configuration is accepted with probability $e^{-\Delta S}$ and rejected; that is $\vec{y} = \vec{x}$ with probability $1 - e^{-\Delta S}$.

The most common implementation is sequential updating of the variables on each time slice by defining $x_i T = x_i + \xi \Delta x$ with ξ uniformaly distributed on the interval $(-\frac{1}{2}, \frac{1}{2})$. Whereas this method is satisfactory for many applications, consider the problem of updating a configuration in which every point of the trajectory is localized in the left well. The cost in action for a variable x_m to cross the barrier from one minimum to the other in a single step is $\Delta S \sim 4m/\varepsilon$. Once x_m has crossed the barrier there is no additional cost for each subsequent variable to cross, and the total probability of creating an instanton in this way in a single sweep is proportional to $(\beta/\varepsilon) e^{-(4m/\varepsilon)}$ compared to the physical probability $(4\sqrt{2}/\sqrt{\pi})(8/m)^{1/4} \beta e^{-(4/3)\sqrt{2m}}$. For extremely large values of the time step, $\varepsilon \gtrsim \sqrt{m}$, there is no problem, and the equilibrium Metropolis distribution correctly samples configurations of all numbers of instantons.[15] However, for $\varepsilon \ll \sqrt{m}$, as required to adequately approach the continuum limit for problems of physical interest, the formation of instantons in a single step is exponentially inhibited.

Generation of instantons by a sequence of small steps of order $\Delta x \sim \sqrt{2\varepsilon/m}$ is strongly inhibited by the fact that the sequential changes Δx_i at each time slice are totally uncorrelated. In the absence of the barrier, the distance would only increase as $\sqrt{N}$ where N is the number of steps, and with the barrier the evolution becomes heavily biased toward remaining in the original well. Hence, the net effect is that as $\varepsilon \to 0$ the Markov

walk gets stuck in a local minimum with a fixed number of instantons and does not sample the full space in any realistic computation time. Note that this disease is in no way restricted to the Metropolis algorithm. Any microreversible method in which changes at sequential points are uncorrelated—for instance, solution of the Langevin equation—suffers a similar fate.

Within a sector os specific instanton number, sequantial updating efficiently sums fluctuations around the classical path, even when higher than quadratic terms are important. Typical results are shown in Fig. 2. Note particularly that although the average behavior of the trajectories closely follows the instanton in the classically forbidden region, the average is displaced away from the minima in the rest of the space, reflecting significant contributions of anharmonic terms. Thus, we conclude that sequential updates are good at summing local fluctuations around stationary paths, but may fail in producing the global changes required to sample all sectors of the trajectory space.

Once the essential problem with sequential updates has been recognized, it is possible to introduce several generalizations to include instanton physics. One alternative for the symmetric function $F(\vec{x} \to \vec{y}^T)$ is

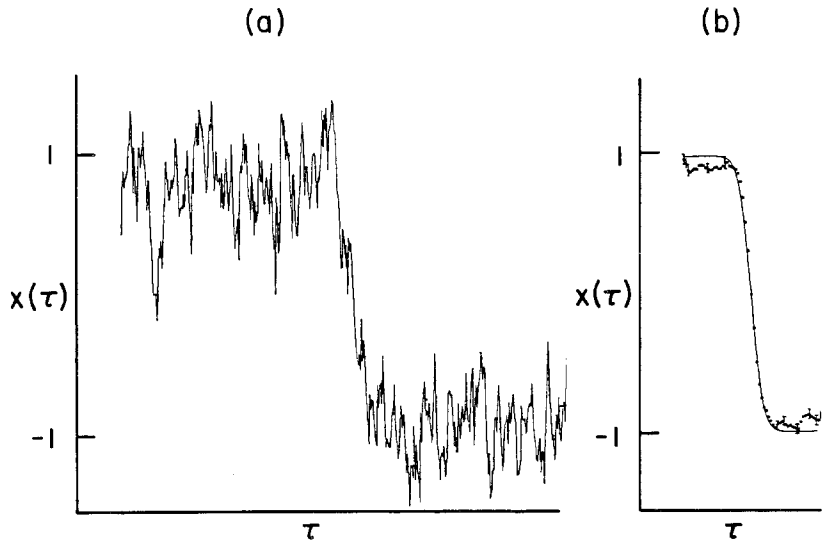

Fig. 2. Trajectories in the one-instanton sector. The left panel shows a typical configuration. The right panel compares the average over many such trajectories in the frame on the instantons (solid points) with the classical instanton (solid curve).

to define the following correlated additive trial move for the entire trajectory

$$x_i^T = x_i + \sigma f_i \qquad \sigma = \pm 1 \tag{3.10}$$

Here, f_i is some global change defined on all the time slices and σ is a random variable with value ± 1. In order to make the move reversible, f must be randomly added and subtracted, with the disadvantage that half the moves are thereby sure to be rejected. A physical choice for f in calculating the trace in a double well is the two-instanton configuration sketched in Fig. 3. Here $f_i = \tan h\gamma(\tau_i - \tau_s) + \tan h\gamma(\tau_l - \tau_i) - 1$. The cost in action for such a global change is distributed around the classical result and assures that the equilibrium distribution of instantons is built up. Note that if the positions x_s and x_l are also picked randomly, subsequent updates will change the instanton number by ± 2 and distribute the instantons randomly.

A second option is a multiplicative move of the form

$$P(\vec{x} \to \vec{y}) = \frac{1}{1 + \prod_i \alpha_i}\left[\prod_i \delta\left(x_i - \frac{y_i}{\alpha_i}\right) + \prod_i \alpha_i \delta(x_i - \alpha y_i)\right] \tag{3.11}$$

Note that for a general scale change, the weight factors are required for symmetry. For the present case, we may use $\alpha = -1$ for a sequence of points of arbitrary length, thereby reflecting them into the opposite well. For small ε, one must also include a smooth function across the barrier.

Finally, in addition to the introduction of collective moves, one always has the option of using importance sampling. We define a function $N(\vec{x})$ which counts the number of instantons in a configuration, and write the tautology

$$\int d\vec{x}\, \mathcal{O}(\vec{x})\, e^{-S(\vec{x})} = \int d\vec{x}[\mathcal{O}(\vec{x})\, e^{-\alpha N(\vec{x})}]\, e^{-[S(x) - \alpha N(\vec{x})]} \tag{3.12}$$

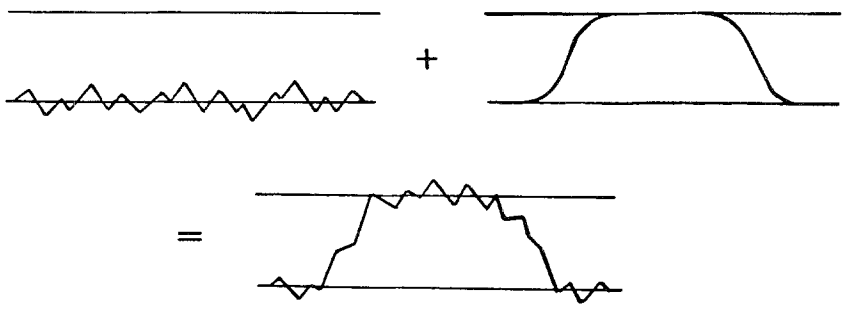

Fig. 3. The effect of adding a two-instanton trial move to a trajectory localized in a single well.

By adjusting α, one can make the acceptance of instantons in the Metropolis updates arbitrarily desirable and thus control the average number of instantons. Although the extraneous factor is exactly divided out in evaluating observables, if the quantity of interest is dominated by multi-instanton configuration, the technique lives up to its name by preferentially sampling the space in the "important" regime. Note also that the definition of an instanton doesn't need to be absolutely precise: as long as $N(\vec{x})$ counts configurations in the desired sector, it will introduce configurations in this sector that subsequently properly equilibrate. Using these techniques, it is straightforward to calculate the energy splitting in a double well (3.6); detailed results may be found in Ref. 14.

We now address each of the steps required to calculate the lifetime of a metastable state in a potential of the form shown in Fig. 1. Although every step may be carried out equally well using guided random walks, at this conference it is appropriate to use the Metropolis algorithm to sample the action. First we must adjust the boundary a to render V_L and V_R degenerate.

Because difference expressions for the kinetic energy are subject to large variance, it is preferable to use the virial theorem to replace $\langle T \rangle$ by a local expression. Retaining the surface terms arising from the nonhermaticity of the boundary condition, we obtain, for an arbitrary x_0

$$\begin{aligned} \langle \psi | \, [H, p(x-x_0)] \, | \psi \rangle &= 2\langle T \rangle - \langle (x-x_0) \, V'(x) \rangle \\ &= (\hbar^2/2m)(x-x_0) \, |\psi'|^2 |_{-\infty}^{a} \end{aligned} \tag{3.13}$$

Hence, the presence of a single hard wall may be accommodated by selecting $x_0 = a$, and the energy may be written

$$E = \langle V + \tfrac{1}{2}(x-a) \, V' \rangle \tag{3.14}$$

The derivative dE/da is needed for two reasons: to improve the precision of determination of a and to determine the density of states in factor contributing to γ. An infinitesimal rescaling of the Schrödinger equation of the form $y = [a|(a+\delta_a)] \, x$ yields

$$\left\{ -\frac{1}{2m[1+(\delta_a/a)]^2} \frac{\partial^2}{\partial y^2} + V\left[\left(1+\frac{\delta_a}{a}\right) y\right] \right\} \psi + E(a+\delta_a)\,\psi \tag{3.15}$$

so that, using the virial theorem

$$\frac{dE}{da} = \left\langle \frac{2}{a} T + \frac{x}{a} V' \right\rangle = \left\langle \frac{(2x-a)}{a} V'(x) \right\rangle \tag{3.16}$$

Finally, it is desirable to incorporate the hard wall boundary condition in the path integral to the same accuracy in ε as the rest of the approximations. Although for smooth potentials, the infinitesimal evalution operator $\exp -(m/2\varepsilon)(x_n - x_{n-1})^2 - \varepsilon\{[V(x_{n-1}) + V(x_n)/2]\}$ produces errors in observables of order ε^2; for a hard wall the wave function is of order $\sqrt{\varepsilon}$ errors in observables. The cure is to generate the path integral using states that are odd about $x = a$, with the result

$$\begin{aligned}(\langle x_n| - \langle 2a - x_n|)\, e^{-\varepsilon H}\, |x_{n-1}\rangle \\ = (2m\pi/\varepsilon)^{1/2}\, e^{-(m/2\varepsilon)(x_n - x_{n-1})^2} \\ \times e^{-(\varepsilon/2)[V(x_n) + V(x_{n-1})]}(1 - e^{-(2m/\varepsilon)(a - x_n)(a - x_{n-1})})\end{aligned} \tag{3.17}$$

This antisymmetrization just subtracts off the Green's function corresponding to the first image across the boundary, and one can explicitly verify for the first odd state of the harmonic oscillator that this leading error is of $\mathcal{O}(\varepsilon^2)$ when images are included.

Finally, all these results may be combined to determine the lifetime of a metastable state. A test problem of the form shown in Fig. 1 was constructed from continuously connected parabolas. The energy splitting for the corresponding degenerate well was obtained as shown in Fig. 4 from $\Delta E_{\text{eff}} = (2/\beta) \tan h^{-1} R$, where R is the ratio defined in (3.3) and a correc-

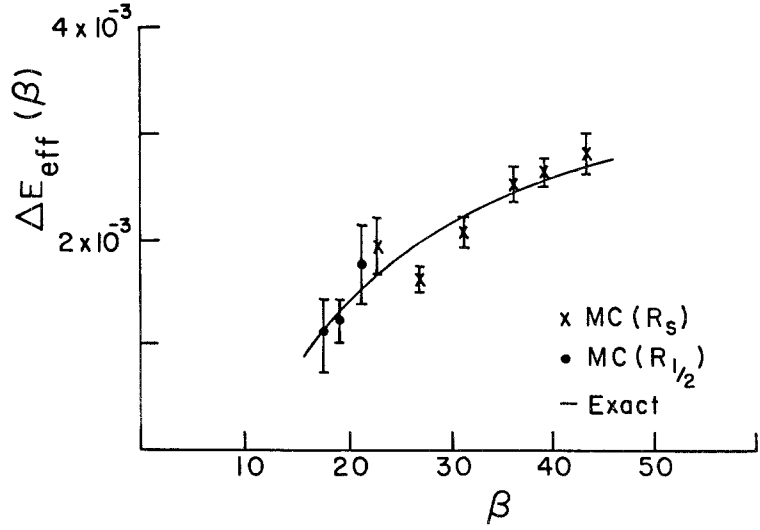

Fig. 4. Monte Carlo calculation of the effective gap $\Delta E_{\text{eff}}(\beta)$ governing the lifetime of a metastable state.

tion factor arising from the fact that $\langle 1|\phi_L\rangle/\langle 0|\phi_L\rangle$ and $\langle 1|\phi_R\rangle/\langle 0|\phi_R\rangle$ is unequal in magnitude for an asymmetric well. The result $\Delta E_{mc} = (3.85 \pm .22) \times 10^{-3}$ is in excellent agreement with the exact result $\Delta E = 3.82 \times 10^{-3}$. Including the density of states, factor dE/da yields a final Monte Carlo result for the inverse lifetime $\gamma_{mc} = (3.4 \pm .41) \times 10^{-4}$, in good agreement with the exact result $\gamma = 3.32 \times 10^{-4}$. Since previous experience with similar problems indicates that accuracy is not seriously degraded in going from one-body test problems to a many-body problem of the form treated in this work, and since only a modest sample size $N \sim 10^5$ was required for this calculation, it is reasonable to expect this approach to be applicable to the many-body problem.

4. PEDAGOGICAL NUCLEAR MODELS

Since, by the arguments presented in this introduction, Monte Carlo calculations of realistic nuclear systems are not yet feasible, the studies presented here address simplified pedagogical models. By providing solutions which are exact to within controlled statistical errors, path integral Monte Carlo calculations offer the unique opportunity to study specific aspects of nontrivial many-body problems without the usual ambiguities associated with crude, uncontrolled many-body approximations. The most essential simplification of the two models discussed below is the restriction to one spatial dimension, which enables us to evaluate Feynman path integrals for many fermions in an ordered subspace with no delicate cancellations arising from antisymmetry.

Nuclear Potential Model

In order to construct a one-dimensional model as relevant as possible to nuclear physics, it is desirable to define a saturating system interacting with a two-body potential exhibiting the qualitative behavior of the nuclear force. To define the potential quantitatively, it is useful to require that relevant dimensionless ratios be comparable in one and three dimensions. The fundamental length scale in a saturating system is specified by the saturation density ρ_0, and so by denoting the dimension by D we define $l_0 = \rho_0^{-1/D} = 1.89$ fm in three dimensions. To within uninteresting geometrical constants, l_0 specifies the characteristic distance between particles. The Schrödinger equation may then be reduced to dimensionless form by measuring all lengths in units of l_0 and energies in units of $E_0 = \hbar^2/ml_0^2 = 11.6$ MeV. The potential used in this work was defined in Ref. 3 such that the scaled binding energy per particle, $(E/A)/E_o$, fermi gas kinetic energy per particle, $(T/A)/E_0$, core radius, r_0/l_0, and maximum

attraction, $V_{\max}/E_o$, are roughly comparable to the three dimensional values.

A crucial consideration in practical calculations is extrapolation of observables as the time step $\varepsilon \to 0$. The evolution operator used in this work is formally accurate to order ε^2, but one still needs to know how small ε must be in order for quadratic convergence to set in. As argued in the introduction, since the Gaussian factor confines $\Delta x \sim \sqrt{\varepsilon}$ and the smallest characteristic scale of variation of the potential is 0.2, one would expect to see convergence at $\varepsilon \sim (0.2)^2 = 0.04$. From Monte Carlo calculations of the binding energy of nuclear matter, one observes that the heuristic estimate $\varepsilon \sim 0.04$ is quite reasonable and that sufficiently accurate results are obtained using the order of 10^4 to 10^5 independent events. Because of the large values of β required to treat collective motion, fission calculations were carried out using $\varepsilon = .05$. It is often useful to think of the error introduced by finite ε as a renormalization of the bare Hamiltonian, $H_\varepsilon \equiv \ln e^{-\varepsilon(V/2)} e^{-\varepsilon T} e^{-\varepsilon(V/2)}$. Calculated binding energies for 2 to 16 particles are well-reproduced by a semiempirical formula of the form $BE(A) \sim E_0 A - E_s$, where E_0 is the nuclear matter binding energy obtained by placing six or more particles in a cell with periodic boundary conditions and varying the length of the cell.

In order to produce spontaneous fission, a long-range repulsive interaction must be added to the Hamiltonian analogous to the Coulomb interaction. In the present case, the range and strength were adjusted so that a 16-particle system was stable with respect to single-particle emission, and unstable with respect to fission into two, 8-particle fragments, and so that the fission barrier was as high as possible.

Ground-state density distributions for three nuclei with this force are shown in Fig. 5. Note that, due to the long-range repulsion, the average interior density is slightly lower than the saturation density $\rho_0 = 1.25$ (defined without this repulsion). The quantum density fluctuations are especially interesting. In the two-body system, antisymmetry forces the density to vanish at the origin, and the size of the low-density region is increased by the repulsive core. In nuclei as large as $A = 8$, the density fluctuations are comparable to those arising from single-particle wave functions in a smooth potential well.

It is important to note that as in the case of real nuclei, the one-dimensional model incorporates dynamics on two very different energy scales: short range correlation effects involving very high kinetic and potential energies and collective dynamics including fission at much lower energies.

It is straightforward to generalize the stochastic tunneling calculation for a single degree of freedom in the previous section to the fission of a metastable 16-particle nucleus. A collective fission variable must be iden-

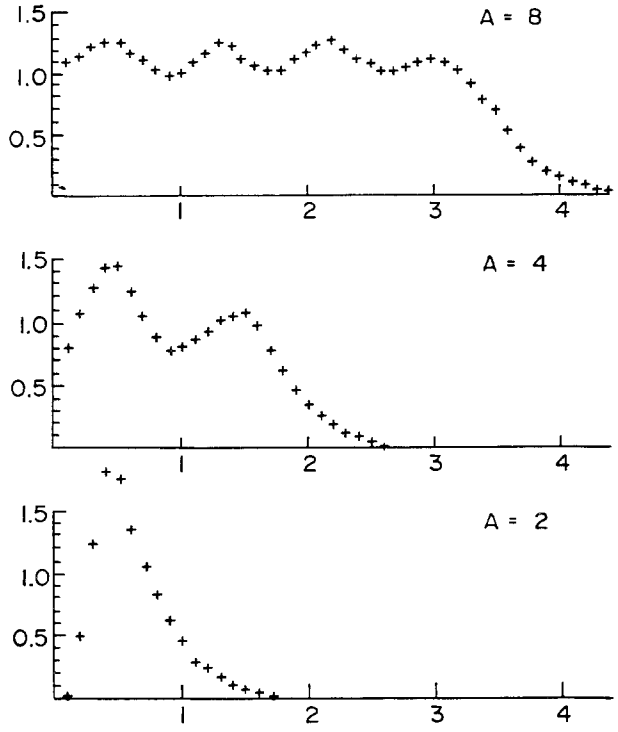

Fig. 5. Ground-state density distributions for two-, four- and eight-particle bound states.

tified for two reasons. To obtain the lifetime from the phase shift in the fission fragment channel, a hard wall forcing a node in the relative wave function must be introduced as in the one-dimensional example. In addition, it is necessary to offer instanton configurations. The ambiguity, in principle, in defining a collective fission variable is no problem, since any definition must reduce to the relative fragment separation at the outer boundary and any reasonable definition which connects the inner and outer local mimima suffices to sample all multiple instanton sectors. In this work, it suffices to let

$$r=\frac{1}{8}\left\{\sum_{i=9}^{16} x_i-\sum_{i=1}^{8} x_i\right\}$$

Because of the simultaneous vanishing boundary conditions at $r=a$ and at all the boundaries $x_{i+1}=x_i$, shifts in the virial theorem cannot eliminate all $|\psi'|^2$ contributions, and the small correction at the boundary $x_8=x_9$ must be calculated explicitly.

Since we have restricted the treatment to single-channel decay, the model must be defined such that only one channel is open. Because the energies of asymmetric fission channels are very close to the symmetric channel, it is convenient to impose the additional symmetry on the problem that all states be symmetric with respect to reflection about the center of mass. This symmetry may be imposed on the mean field theory as well, providing a nontrivial single-channel model for comparing mean-field theory with an exact solution.

To calculate the energies in the inner and outer wells and to calculate the $\langle \phi_L | E^{-\beta H} | \phi_R \rangle$-matrix element pertinent to the fission lifetime, a number of different trial moves were offered in each iteration of the Metropolis algorithm:

1. Sequential updates. The coordinates of x_i^8 for each of the 16 particles on each of 400 time slices were sequentially updated during each sweep. Irrespective of all the other moves, these sequential updates summed the fluctuations around each of the dominant solutions.
2. Dilational modes. The low-energy collective excitations require the greatest number of iterations to be refined out of the ground-state wave function. This refinement takes even longer when sequantial updates rarely present dilations or contractions of the entire system. Thus, equilibrium is significantly accelerated by offering a multiplicative scaling mode $x_i'^n = a x_i^n$ to the lattice as a whole once each iteration.
3. Sequential updates in r. Moves in the single-particle variables x_i, which are small enough to avoid rejection by virtue of the strong repulsive core, are very ineffective in introducing changes in the collective variable r large enough to explore all relevant values of r. Thus, with each iteration, the value of r on each time slice is sequentially updated just like the coordinate of a single particle in a collective well.
4. Instantons in r. Finally, after offering each of the preceeding updates, an additive instanton in r of random length in time is offered. The approximate shape of the instanton was determined from the energy of deformation surface specified by a constrained Hartree-Fock calculation and confirmed by calculating the equilibrium distribution in the one-instanton sector analogous to Fig. 2.

The net result of offering all these alternative moves is a statistically viable evaluation of all the ingredients $E_L, E_R, \partial E_R/\partial a$, and $\langle \phi_L | e^{-\beta H} | \phi_R \rangle / [\langle \phi_L | e^{-\beta H} | \phi_L \rangle \langle \phi_R | e^{-\beta H} | \phi_R \rangle]^{1/2}$ required to calculate the lifetime. An example of a typical contribution to $\langle \phi_L | e^{-\beta H} | \phi_R \rangle$ in the one instanton sector is shown in Fig. 6. Note that the many-body trajectory clearly exhibits separation into two-fission fragments and the

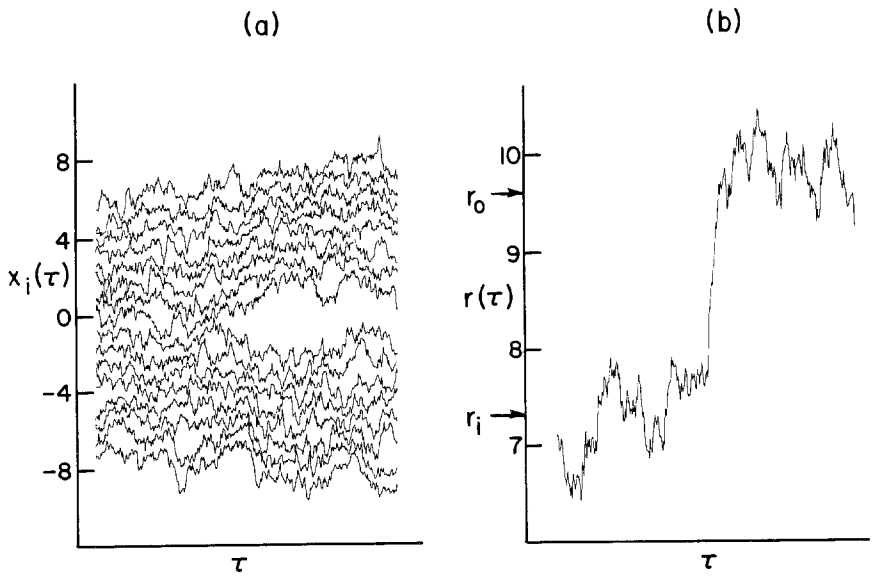

Fig. 6. Typical configurations of the 16-particle system in the one-instanton sector. The left-hand panel shows the coordinates of each of the 16 particles on 400 time slices and the right-hand panel shows the corresponding trajectory of the collective coordinate.

corresponding trajectory for the collective coordinate has the same behavior as the single-particle example in the preceding section.

The principle result is the fact that the method can be made to work, even for a problem as demanding as this nuclear model containing two significantly different energy scales.

Confining Quark Model

The confining quark model of Ref. 16 provides a convenient system in which to study how certain aspects of nuclear structure arise from underlying quark degrees of freedom. By studying the model in one spatial dimension, it is possible to obtain exact solutions for uniform matter described both in terms of quark and hadronic degrees of freedom and thus explore the complementarity of the two descriptions.[4]

Physically, the model may be thought of as an adiabatic limit in which for any configuration of $2N$ spinless quarks, the color fields instantaneously adjust themselves to form the lowest energy configuration in which N distinct pairs of quarks are connected by flux tubes. Mathematically, the model is defined by specifying a potential energy of the quarks to be

$$V = \min_P \{v(x_{P1} - x_{P2}) + v(x_{P3} - x_{P4}) + \cdots + v[x_{P(N-1)} - x_{PN}]\} \qquad (4.4.1)$$

where the minimum overall permutation selects the lowest energy assignment of pairs. The theory exhibits the desired separability, confinement, and exchange symmetry and is free of Van der Waals interactions. Although finding the optimal pairing in three dimensions entails solution of a nontrivial assignment problem, in one dimension with periodic boundary conditions, the optimal pairing of consecutively labeled quarks either pairs q_{2m} with q_{2m+1} or q_{2m} with q_{2m-1} for all m. Hadrons are composed of two quarks in the simplest version of the model used here, and are thus bosons. The potential $v(x)$ is taken to be quadratic, yielding a quark density in a free nucleon proportional to $x^2 e^{-(x^2/\sqrt{2})}$.

It is instructive to compare observables calculated in this model with the results obtained from an effective Hamiltonian having only hadronic degrees of freedom. As in traditional nuclear physics, a hadron–hadron potential may be defined to reproduce the exact hadron scattering phase shifts, and the many-hadron problem is solved with this potential. We find that a gross property such as the hadronic matter binding energy as a function of density is well-reproduced by this effective Hamiltonian, whereas the quark–quark correlation function and quark momentum distributions, which would be probed in deep inelastic electron scattering, reflect the underlying quark structure.

The phase shifts for the scattering of a two-quark hadron from a two-quark hadron may be solved stochastically below threshold by calculating the ground state of the four-quark system with the appropriate boundary condition on the distance between the centers of mass of the left two quarks and the right two quarks; Monte Carlo results are shown in Ref. 4. Since the phase shifts in this energy range are evidently characterized by a scattering length and an effective range, they are easy to reproduce with a simple local potential $V_N(x) = (52/\sqrt{2\pi})e^{-(x^2/2)}$. Of the two effects which occur for overlapping hadrons—diminuation of the potential interaction energy and increased kinetic energy due to the Pauli principle—the later effect dominates and the interaction is purely repulsive.

The binding energy per quark of uniform nuclear matter is shown in Fig. 7. Stochastic solution of the many-quark problem yields the solid dots, and the many-hadron problem defined by bosons interacting via the phenomenological potential $V_N(x)$ yields the triangular points.

In order to calibrate densities in the one-dimensional model, it is useful to note that the ratio $\bar{\rho}_N/\rho_{NM} = (1.1)^3$, where $\bar{\rho}_N$ denotes the average density in a proton of uniform density and the observed rms charge radius, and $\bar{\rho}_{NM}$ is nuclear matter density. Since the average density of a hadron in the one-dimensional model is $\bar{\rho}_H = 0.5$, a corresponding degree of overlap obtains at a hadronic matter density $\bar{\rho}_{HM} = 0.5/1.4 \sim 0.45$. Thus, we observe from Fig. 7 that up to densities twice that of hadronic matter, the binding

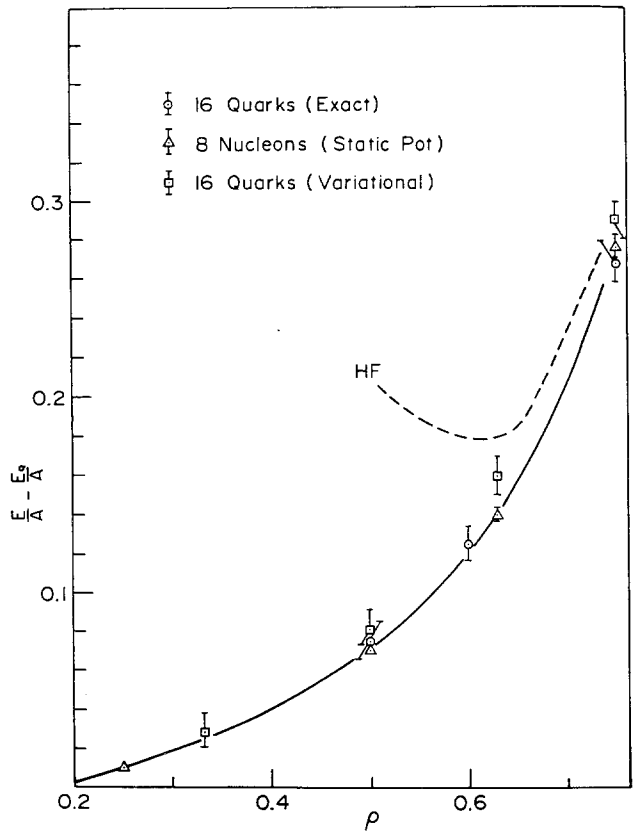

Fig. 7. Monte Carlo calculation of the binding energy per quark of uniform matter calculated with the quark Hamiltonian (circles) and the effective hadron Hamiltonian (triangles).

energy yields no signature of quark substructure or, equivalently, of the breakdown of the descriptions in terms of hadronic degrees of freedom.

A microscopic view of the quark behavior is provided by the quark–quark correlation functions shown in Fig. 8, which specify the probability of finding another quark a distance x from a given quark. The normalization is defined such that at density ρ corresponding to n particles in a periodic box of length L, the integral of the correlation function from 0 to L is $L(n-1)$, thus counting the $(n-1)$ remaining particles. The Fermi gas correlation function then approaches 1 in the interior of the box and approaches zero within range $1/k_F$ of 0 and L as shown by the long dashed lines. At very low density, one would expect the correlation function to look like the undistorted ground state nucleon density at short distances

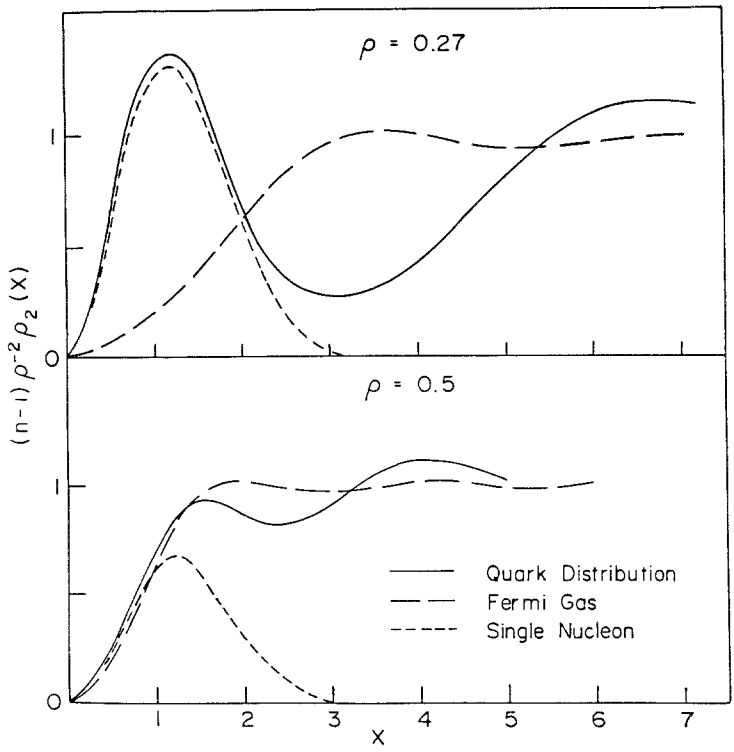

Fig. 8. Quark–quark correlation functions as described in the text.

and approach a constant corresponding to the low-density nucleon gas at large distances. Hence, the appropriately normalized density distributions for a single hadron are also shown in Fig. 9 by the short dashed curves. As observed in the top portion of the figure, at $\rho = 0.27$, roughly half the density of hardonic matter, the quark distribution exhibits the low density behavior of undistorted hadrons. At $\rho = 0.5$, however, corresponding to hadronic matter density, the nucleon correlations have nearly disappeared and the correlation function is close to that of a fermi gas. Note that at this density, the binding energy is still well-represented by the effective hadron–hadron potention. An analogous transition between the hadron momentum distribution and a Fermi gas distribution is observed in the quark momentum distribution. At hadronic matter density, one observes the enhancement at high momentum, enhancement at low momentum, and depletion at intermediate momentum characteristic of the EMC effect.

This provocative coexistence of bulk properties, accurately governed by an effective Hamiltonian containing only hadronic degrees of freedom

while leptonic probes reveal definite signatures of quark substructure, is presently being investigated in more realistic confining models in three dimensions having nucleons comprised of three quarks.[17]

5. SUMMARY AND CONCLUSIONS

We are beginning to learn to exploit the freedom in formulating algorithms to incorporate physics into quantum Monte Carlo calculations. In addition to the familiar use of trial functions to generate guided random walks, I have shown that collective updates in the Metropolis method can incorporate one's understanding of semiclassical instanton solutions in tunneling problems with many degrees of freedom.

Although realistic Monte Carlo calculations of heavy nuclei are presently impractical, the exact solution of pedagogical models can provide useful insight into aspects of both nuclear and subnuclear structure.

In looking to the future, four challenges in particular stand out. One is the infamous fermion sign problem, and we can only hope that the ideas such as those discussed by Kalos and Koonin will eventually bear fruit. The second is calculation of the real-time response function $S(k, w)$. In the case of fission, we were very fortunate that the essential information governing the lifetime in real time could be extracted from the gap, that is, the energy splitting between the two most slowly decaying exponents in imaginary time. The general response function, however, which is required to study the rich data provided by inclusive lepton scattering, has delicate interference effects in real time which thus far have proven impossible to study with Monte Carlo. The third challenge is to find ways to calculate linked rather than unlinked quantities. Finally, we need to learn eventually how to exploit the impressive Monte Carlo studies of lattice gauge theories to answer fundamental questions about the nature of hadronic interactions and the role of quark and gluon degrees of freedom in real nuclei.

ACKNOWLEDGMENT

This work was supported in part through funds provided by the U.S. Department of Energy (D.O.E.) under contract number DE-AC02-76ER03069.

REFERENCES

1. D. M. Ceperley and M. H. Kalos, *Monte Carlo Methods in Statistical Mechanics*, K. Binder, ed. (Springer-Verlag, New York, 1979).
2. S. E. Koonin, *Nuclear Theory 1981*, G. F. Bertsch, ed. (World Scientific, 1981).

3. J. W. Negele, *Proceedings of the International Symposium on Time-Dependent Hartree-Fock and Beyond*, Lecture Notes in Physics, No. 171, K. Geoke and P. G. Reinhardt, eds. (Springer-Verlag, New York, 1982).
4. C. Horowitz, E. Moniz, and J. W. Negele, *Phys. Rev. D* **31**:1689 (1985).
5. J. W. Negele, *Proceedings of "Path Integrals from mev to MeV"* J. Klauder, ed. (Bielefeld, 1985).
6. J. W. Negele, *Rev. Mod. Phys.* **54**:913 (1982).
7. N. Metropolis, A. Rosenbluth, M. Rosenbluth, A. Teller, and E. Teller, *J. Chem. Phys.* **21**:1087 (1953).
8. J. W. Moskowitz, K. E. Schmidt, M. A. Lee, and M. H. Kalos, *J. Chem. Phys.* **77**:349 (1982).
9. D. Ceperley and M. Kalos, private communication; E. L. Pollack and D. M. Ceperley, *Phys. Rev. B* **30**:2555 (1984).
11. J. Langer, *Ann. Phys. (N.Y.)* **54**:258 (1969).
12. A. M. Polyakov, *Nucl. Phys. B* **121**:429 (1977).
13. S. Coleman, in *The Whys of Nuclear Physics*, A. Zichichi, ed. (Plenum, New York, 1977), p. 805.
14. C. Alexandrou, Ph. D. dissertation (MIT, 1985).
15. M. Creutz and B. Freedman, *Ann. Phys.* **132**:427 (1981).
16. F. Lenz, J. T. Longergan, E. J. Moniz, R. Rosenfelder, M. Stingl, and K. Yazaki, *Ann. Phys.* in press.
17. R. M. Panoff, private communication.